A Study of Freight Vehicle Effects on Rail Surface Damage

UK Proprietary 06-003

Submitted to Booz Allen Hamilton, UK
for the Office of Rail Regulation, UK

By John Tunna, Steve Clark,
and Curtis Urban
TTCI(UK), Ltd.
31 May 2006

EXECUTIVE SUMMARY

A preliminary study has been made of the effects of several freight vehicle parameters on rail surface damage. Computer models of the following vehicles were used in the study:

- Class 60 and Class 66 locomotives
- FSA Wagon with Y25 bogies and P10 wheel profiles
- HTA wagon with NACO Swing Motion bogies and P8 wheel profiles
- HAA wagon (2-axle leaf spring) with P5 wheel profiles

The study showed the following parameters have a relatively small effect on Rolling Contact Fatigue (RCF) damage:

- Unsprung mass
- Bogie yaw inertia
- Longitudinal and Lateral primary clearance
- Bogie Spacing
- Axle Spacing
- Side-bearing clearance

The following parameters were found to have a significant effect on RCF damage and should be considered in any further analysis:

- Curve distribution
- Track quality
- Conicity
- Vehicle type
- Empty or loaded
- Traction and braking

Since many of these parameters vary between routes on the network, it is concluded that route-based analysis of rail surface damage by freight vehicles would give much more accurate results than applying network average conditions.

TABLE OF CONTENTS

1.0 INTRODUCTION

In preparation for a possible review of freight access charges, the Office of Rail Regulation (ORR) has asked TTCI(UK) Ltd., a subsidiary of Transportation Technology Center, Inc., to perform a scoping study on rail surface damage caused by freight vehicles. This report describes the variety of freight vehicles in operation on Network Rail controlled infrastructure. The results of modelling on a sub-set of these vehicles are presented. Recommendations are made for further work that would be necessary to evaluate freight's contribution to track costs.

2.0 UK FREIGHT VEHICLES

2.1 Naming Convention

Freight vehicles are referred to by Total Operating Processing System (TOPS) codes.

Locomotive TOPS codes are classified by a numerical allocation scheme that identifies their class designation. The class designation indicates the power supply, and in the case of diesel locomotives, the horsepower range.

Table 1. Freight Locomotive Classes

Class	Power
01-14	0-799 hp, diesel
15-20	800-1,000 hp, diesel
21-31	1,001-1,499 hp, diesel
32-39	1,500-1,999 hp, diesel
40-54, 57	2,000-2,999 hp, diesel
55-56, 58-69	3,000+ hp, diesel
70-80	DC electric and dual DC/diesel
81 onwards	AC electric

Wagons follow a three letter TOPS classification scheme. The following explains the meaning of each letter:

First letter – main type of wagon:

B Bogie steel
C Covered bulk
F Flat wagon
H Hopper
J Private owner
M Mineral wagon
P Private owner
R Railway operating

S 2-axle steel
Y Service (bogie freight)
Z Service (2-axle freight)

Second letter – subdivision of main type

Third letter – brake type:

A Air brake
B Air brake through vacuum pipe
O No brake (hand only), unfitted
P No brake (hand only), vacuum pipe only
Q No brake (hand only), air pipe only
R No brake (hand only), dual air and vacuum pipe
V Vacuum brake
W Vacuum brake through air pipe
X Dual brake (air and vacuum)

There is actually a fourth character in the TOPS codes for freight wagons that identifies specific variations of wagons. The fourth letter is not used on the actual wagons, but only appears on computer records and official diagrams.

In addition to their TOPS codes, engineering department wagons are commonly known by marine names such as “Salmon” and “Mermaid.”

2.2 Usage Charging Categories

The ORR currently separates freight vehicles into the following eight categories for the purpose of calculating track access charges:

1) Freight locomotives
2) Four wheel (2-axle) wagon with pedestal type suspension
3) Four wheel (2-axle) wagon with leaf springs, friction damped
4) Wagon equipped with three piece bogie
5) Bogie wagon with enhanced three piece bogie (e.g. “swing motion” or parabolic four wheel wagon)
6) Basic wagon with primary springs (e.g. Y25 suspension type)
7) Wagon equipped with enhanced primary springs (i.e., low track force bogies, TF25 types or “axle motion”)
8) Wagon equipped with enhanced primary springs and steering

3.0 SELECTION OF VEHICLES FOR MODELLING

There are over 500 TOPS codes identifying different freight locomotives and wagons that operate on the infrastructure controlled by Network Rail, if all the variations of wagons are considered. However, the majority of vehicle miles are covered by relatively few types of wagons and locomotives.

Data from year 2005 was obtained from the TOPS system to determine which vehicles operate the greatest mileage on the UK railway network.

Table 2 presents the top five locomotive types in terms of miles travelled on the network. The Class 66 locomotive is clearly the most highly utilized locomotive on the network with approximately 64 percent of the total locomotive miles travelled. Combined, the Class 66 and Class 60 locomotives comprise almost 80 percent of all locomotive miles travelled on the network.

Table 2. Freight Locomotives Most Utilized in 2005

Rank	Class	Miles of Operation	Power	Percent of Total Miles	Cumulative Percent
1	66	21,091,831	Diesel Locomotive	64.3	64.3
2	60	4,918,012	Diesel Locomotive	15.0	79.3
3	92	1,581,502	Electric Locomotive AC	4.8	84.1
4	86	1,319,655	Electric Locomotive AC	4.0	88.1
5	90	790,212	Electric Locomotive AC	2.4	90.5

Table 3 presents the bogie types that comprise 80 percent of all loaded miles on the network. This shows that the Y25 bogie is the most utilized bogie in terms of loaded miles travelled, followed by the single axle with leaf springs and the NACO Swing Motion bogie. These three bogie types comprise almost 60 percent of the total loaded vehicle miles travelled on the network.

Table 3. Bogie Utilization for 80 Percent of Total Loaded Miles (2005)

Bogie Type	Miles of Loaded Operation	Percent of Total Miles	Cumulative Percent
Y25 (all variants)	103,556,956	29.9	29.9
Single Axle Leaf Spring	58,013,606	16.7	46.6
NACO Swing Motion bogie	41,125,622	11.9	58.5
Low Track Force (all variants)	29,547,986	8.5	67.0
Unknown	15,738,406	4.5	71.6
Single Axle Coil Spring	11,914,761	3.4	75.0
various (mixed wagon types)	7,251,390	2.1	77.1
Y33	4,461,452	1.3	78.4
Gloucester (all variants)	3,965,168	1.1	79.5
Y31	2,482,106	0.7	80.3

Table 4 presents the bogie types that comprise 80 percent of all empty miles on the network. Although there are some differences between the loaded and empty utilizations, there is general consistency with the Y25, single axle with leaf springs, and NACO Swing Motion bogie being the most utilized bogies in terms of empty miles travelled.

Table 4. Bogie Utilization for 80 Percent of Total Empty Miles (2005)

Bogie Type	Miles of Empty Operation	Percent of Total Miles	Cumulative Percent
Single Axle Leaf Spring	49,675,421	23.9	23.9
NACO Swing Motion	35,115,947	16.9	40.8
Y25 (all variants)	31,927,008	15.3	56.1
Low Track Force (all variants)	17,117,836	8.2	64.3
Single Axle Coil Spring	13,488,603	6.5	70.8
various (mixed wagon types)	10,114,025	4.9	75.7
Gloucester (all variants)	4,999,256	2.4	78.1
Unknown	2,239,736	1.1	79.2
Y31	1,318,345	0.6	79.8
NACO Super C	994,108	0.5	80.3

Figure 1 presents this same data in graphical format for both loaded and empty wagon miles and shows that for all cases, the Y25 (the single axle with leaf springs and the NACO Swing Motion bogie) operate the most miles.

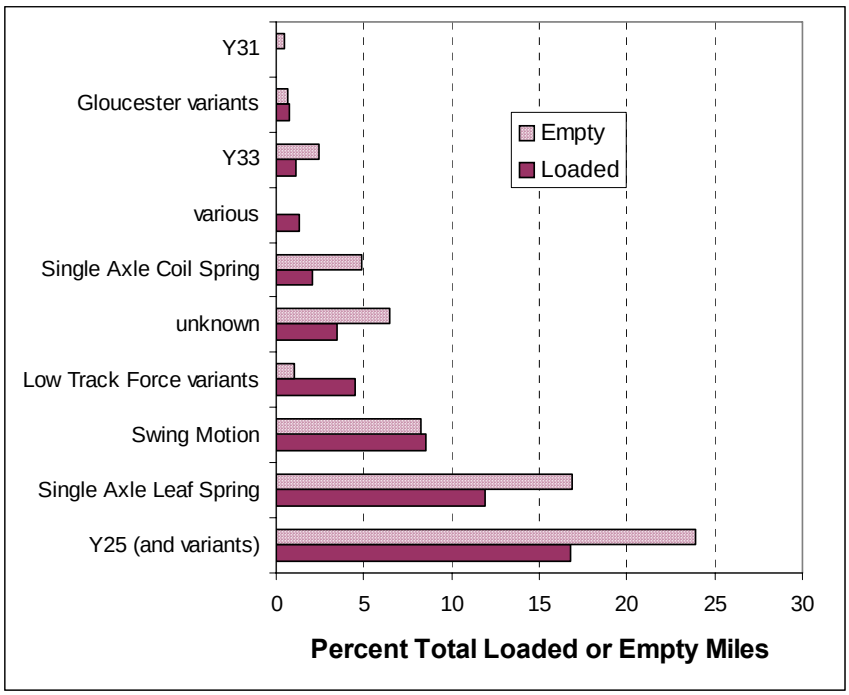

Figure 1. Percent of Miles Travelled by Bogie Type, Empty and Loaded Wagons (2005)

The full list of freight locomotives and the lists of wagons and bogies that comprise the 80th percentile utilization are presented in Appendix A.

The choice of freight vehicles to analyse was based on the utilization of vehicles in terms of miles travelled and the availability of models. Based on the information derived from the analysis of locomotive and vehicle miles travelled and the availability of the models, the following vehicle types were selected for this scoping analysis of the effect of freight vehicles on rail surface damage.

Locomotives:

- Class 60 locomotive / rigid frame 3-axle bogie / P8 wheel profile
- Class 66 locomotive / radial steering 3-axle bogie / P8 wheel profile

Wagon/Bogie Combinations:

- FSA Wagon / Y25 bogie / P10 wheel profile
- HTA Wagon / NACO Swing Motion bogie / P8 wheel profile
- HAA Wagon / Single-Axle Leaf Spring / P5 wheel profile

These vehicles and bogies are illustrated in Figures 2 through 6. Figure 6 is credited to Gareth Bayer, editor of "Wagons on the Web," and Kevin Bruce. Mr. Bayer's website can be found at www.garethbayer.co.uk/wotw.

Figure 2. Class 60 Locomotive

Figure 3. Class 66 Locomotive

Figure 4. Y25 Bogie

Figure 5. NACO Swing Motion Bogie

Figure 6. HAA Wagon with Single Axle Leaf Spring Suspension

The freight vehicles modelled cover usage charging categories 1, 3, 5, and 6 (see Section 2.2).

A typical modern multiple unit passenger vehicle was also modelled for comparison with the freight vehicles.

4.0 MODELLING PROCEDURE

Vehicle dynamic simulations were performed using NUCARS®. Information on the dimensions and masses of the vehicles is given in Appendix B.

4.1 Inputs

The track inputs were a set of right-hand curves with radii, cants, and speeds as shown in Table 5. Vehicle speed was constant at the balance speed for each curve unless limited by the maximum allowable speed of the particular vehicle being modelled.

Table 5. Details of Modelled Curves

Curve No.	Radius (m)	Track Cant (mm)	Speed (km/hour)	Speed (miles/hour)
1	400	150.0	71.2	44.3
2	600	150.0	87.3	54.2
3	800	137.8	96.6	60.0
4	1,000	110.2	96.6	60.0
5	1,200	91.8	96.6	60.0
6	1,400	78.7	96.6	60.0
7	1,600	68.9	96.6	60.0
8	1,800	61.2	96.6	60.0
9	2,000	55.1	96.6	60.0
10	2,200	50.1	96.6	60.0
11	2,400	45.9	96.6	60.0
12	2,600	42.4	96.6	60.0
13	2,800	39.4	96.6	60.0
14	3,000	36.7	96.6	60.0
15	4,000	27.6	96.6	60.0
16	5,000	22.0	96.6	60.0
17	6,000	18.4	96.6	60.0
18	10,000	11.0	96.6	60.0

Track roughness was taken from track recording coach measurements on a slow line used by freight traffic. The standard deviations of vertical and lateral track geometry (70m filter) were 3.6mm and 3.1mm respectively. This track geometry is representative of average track in speed band 7.[1]

The P10 and P8 profiles used in the simulations were typical worn examples from a database of measured profiles. The P5 profile was as designed.

Measured high and low rail profiles were used for all the cases studied. These were taken from a 618m radius curve.

The coefficient of friction between the wheel and rail was assumed to be 0.45 in all cases. This value was chosen to be consistent with other recent investigations into rail surface damage.

4.2 Outputs

Table 6 lists the outputs from the simulations. These outputs were produced for each axle and wheel in the vehicle.

Table 6. Modelling Outputs

Component	Output	Symbol
Bogie	Warp Displacement	
Bogie	Rotation Displacement	
Axle	Yaw Displacement	
Axle	Lateral Displacement	
Wheel/Rail	Normal Force	P
Wheel/Rail	Longitudinal Force	T_x
Wheel/Rail	Lateral Force	T_y
Wheel/Rail	Longitudinal Creepage	γ_x
Wheel/Rail	Lateral Creepage	γ_y
Wheel/Rail	Spin Creepage	
Wheel/Rail	Contact Angle	
Wheel/Rail	Contact Area	
Wheel/Rail	Contact Stress	
Wheel/Rail	Contact Position	

4.3 Post-processing

The lateral and longitudinal tangential forces and creepages were combined to give a continuous output of $T\gamma$ using Equation 1. Note that to be consistent with other investigations into rail surface damage[2] the spin moment and spin creepage terms are not included.

$$T\gamma = T_x\gamma_x + T_y\gamma_y \qquad (1)$$

Figure 7 shows the AEAT damage function[2] used to calculate a continuous output of rail surface damage. The average rail surface damage over the body of the curve was then computed. This is the output that was used later to compare results from the different simulations.

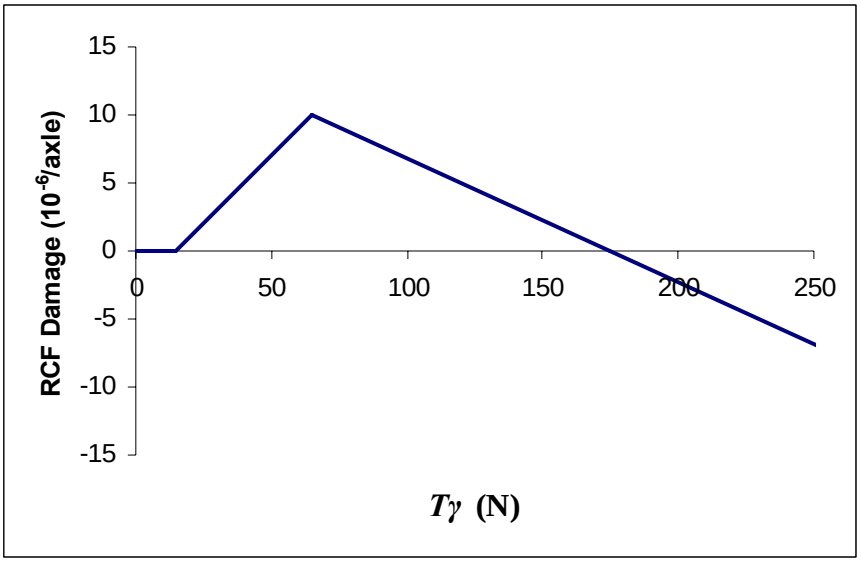

Figure 7. AEAT ($T\gamma$) Damage Function

An alternative method of post-processing the results would have been to calculate the average value of $T\gamma$ on the curve and convert this to RCF damage. A comparison between the two methods is presented later in this report.

4.4 Parametric Variations

The parameters listed in Table 7 were varied.

Table 7. Parametric Variations

Parameter	Variations
Conicity	Low, Normal, High
Unsprung Mass	Normal ± 10%
Bogie Yaw Inertia	Normal ± 10%
Primary Longitudinal Clearance	Tight, Normal, Wide
Primary Lateral Clearance	Tight, Normal, Wide
Primary Yaw Stiffness	Low, Normal, High
Axleload	Empty, Half Loaded, Loaded
Bogie Spacing	Normal ± 10%
Axle Spacing	Normal ± 6%
Side Bearing Clearance	Solid, Tight, Normal, Wide
Traction	None, Full
Braking	None, Normal Service
Track Geometry	V. Good, Good, Average, Poor, V. Poor

Not all the vehicles modelled had the full set of parameters varied.

5.0 RESULTS

More than 2,700 NUCARS® runs were performed for this study. Only the results that produced noteworthy differences in rolling contact fatigue damage are discussed in detail.

5.1 Post-processing Alternatives

Figure 8 shows a typical distance history of $T\gamma$. In this example the vehicle is the HTA with NACO Swing Motion bogies and P8 wheel profiles, the speed is 60 miles/hour and the curve radius is 1,000m. The body of the curve extends from 250 to 650m.

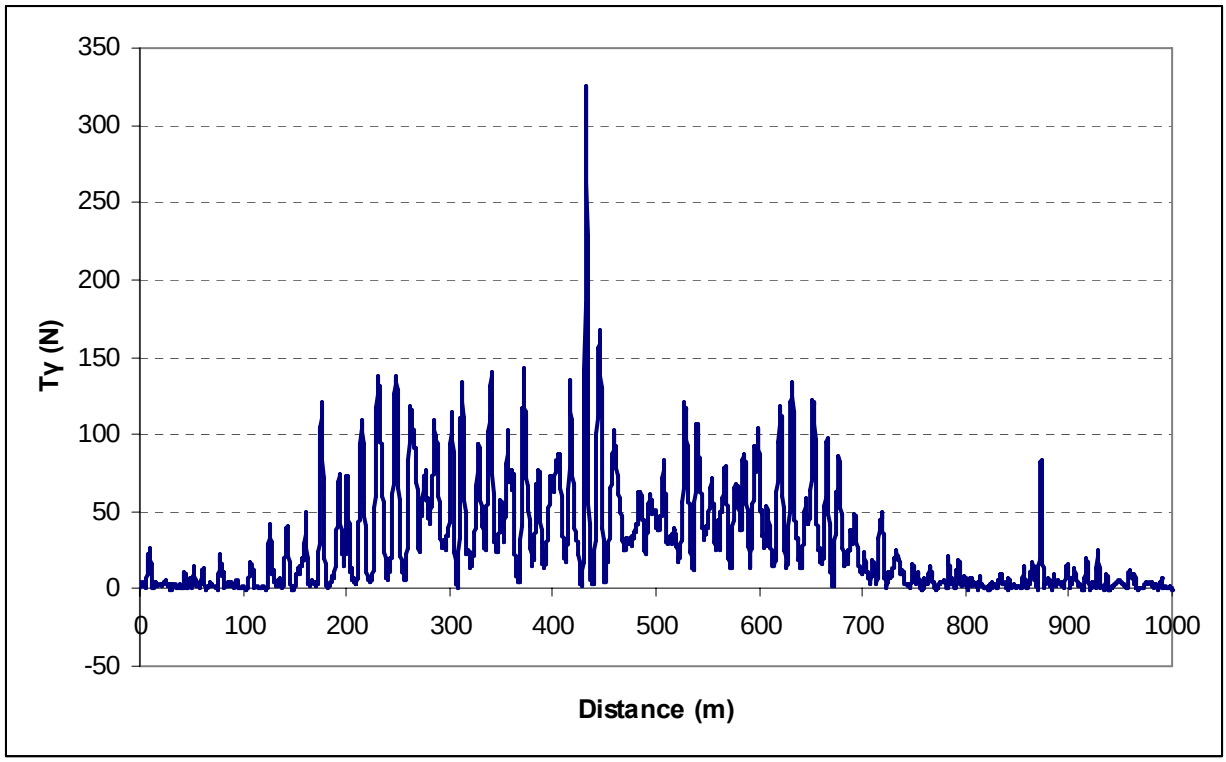

Figure 8. Example $T\gamma$ from High Rail, Lead Axle of the HTA wagon with NACO Swing Motion Bogies

$T\gamma$ can be seen to increase through the first transition, vary about approximately 50N in the body of the curve and reduce over the transition back to straight track. The variation in $T\gamma$ is caused by perturbations in track geometry. There is a large lateral misalignment at 430m, which causes a large dynamic $T\gamma$.

Figure 9 shows the distance history of damage calculated from the $T\gamma$ shown in Figure 8 using the damage parameter shown in Figure 7.

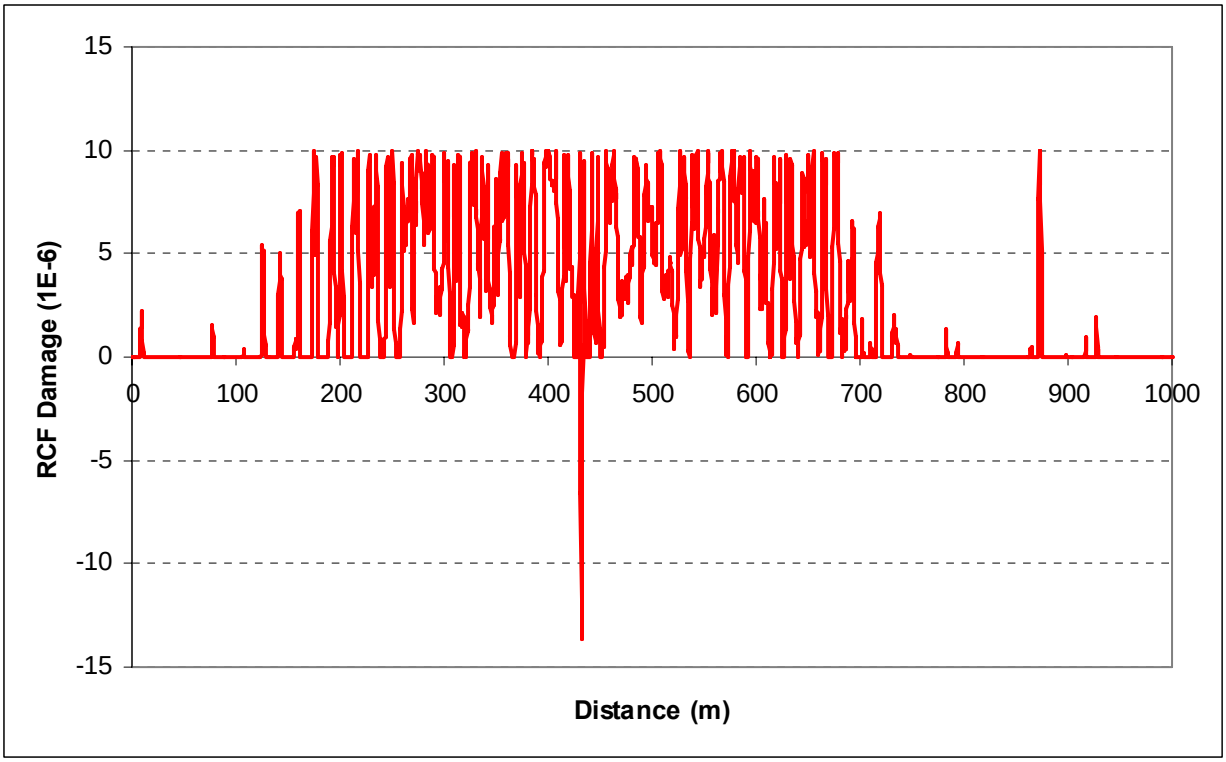

Figure 9. Example RCF Damage from High Rail, Lead Axle of the HTA Wagon with NACO Swing Motion Bogies

At the start of the simulation $T\gamma$, is generally less than 15N and no RCF damage is expected. Damage occurs on the transition and in the curve as $T\gamma$ increases. The maximum RCF damage per wheel pass is 10^{-5} (i.e., 10×10^{-6}), which results from a $T\gamma$ of 65N. The large value of $T\gamma$ at 430m causes wear, which is shown as negative damage.

The average RCF damage in the body of the curve (between 300 and 600m) is 4.94×10^{-6}. Thus, after approximately 200,000 load cycles, half of the high rail in the curve should have developed visible RCF damage.

An alternative method of calculation would be to take the average $T\gamma$ in the body of the curve from Figure 8, which is 54.3N, and use the damage function to calculate a RCF damage of 7.87×10^{-6}. This alternative method overestimates the RCF damage and can produce an average RCF damage of 10^{-5} for the curve. The first method is considered more representative of the RCF damage distribution along the curve. It has been used for all the results that follow in this report.

5.2 Curve Radius

Figure 10 shows that variation of average RCF damage with curve radius for the base case NACO Swing Motion bogie. The results are for the outside wheel of the leading axle.

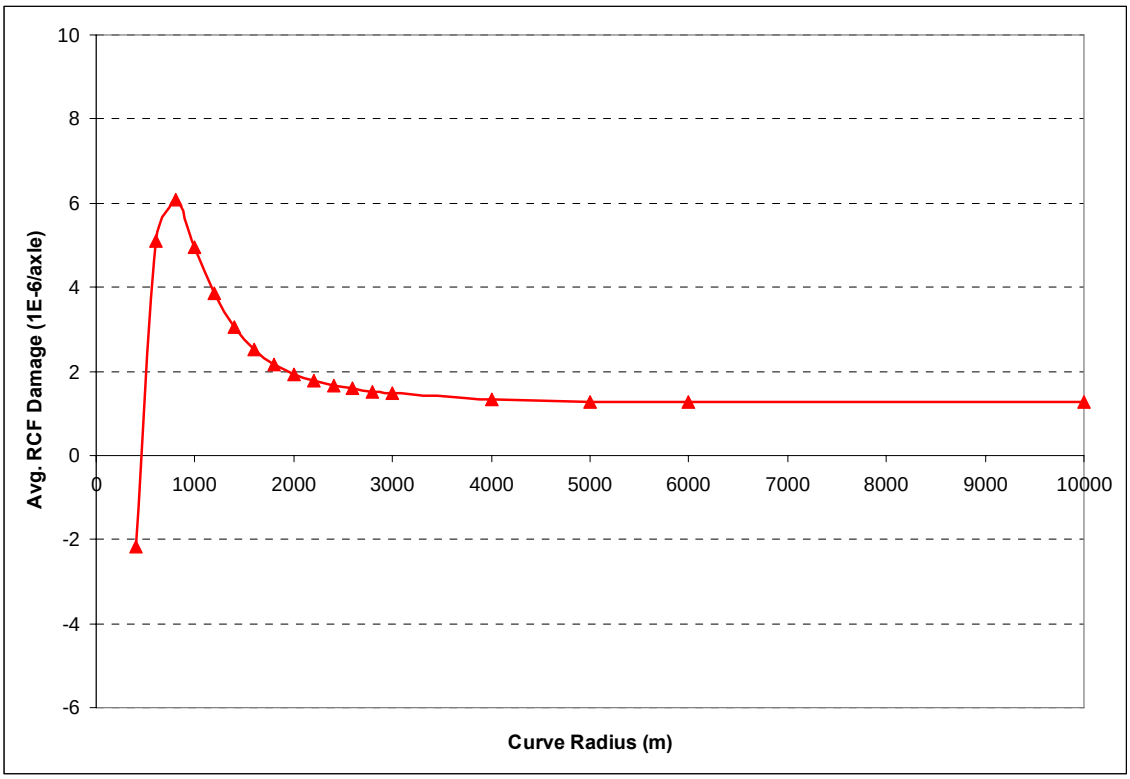

Figure 10. Variation of RCF Damage with Curve Radius – Base Case NACO Swing Motion Bogie, Outside Wheel Lead Axle

When the radius of curvature is large the creepages and creep forces are relatively small. The resulting $T\gamma$ produces little RCF damage. When the radius of curvature is small (e.g. 400m) large creepages and creep forces are produced. The resulting $T\gamma$ is large enough to cause wear and not RCF – hence the negative value shown in Figure 10.

At some intermediate curve radius, a maximum occurs in the RCF damage. In the example of Figure 10, this maximum occurs at 800m curve radius. On this curve the $T\gamma$ values fall close to the peak in the RCF damage function shown in Figure 7.

It can now be seen that the degree of RCF damage a vehicle produces depends on the distribution of curves on the route over which it operates. If, in the example above, the vehicle operated over a route with curves larger than 3,000m radius, very little RCF would be produced. If all the curves were less than 500m radius then only wear would be produced. From the point of view of RCF damage, the worst kind of route for this particular vehicle would be one with curves in the range 600 to 1,200m radius.

Figure 11 shows the distribution of curves on Network Rail controlled infrastructure. Distributions on individual routes may vary significantly from the network total. When comparing RCF damage from different types of vehicles and when assessing track access charges, it is important to account for the curvature distribution of the route in question.

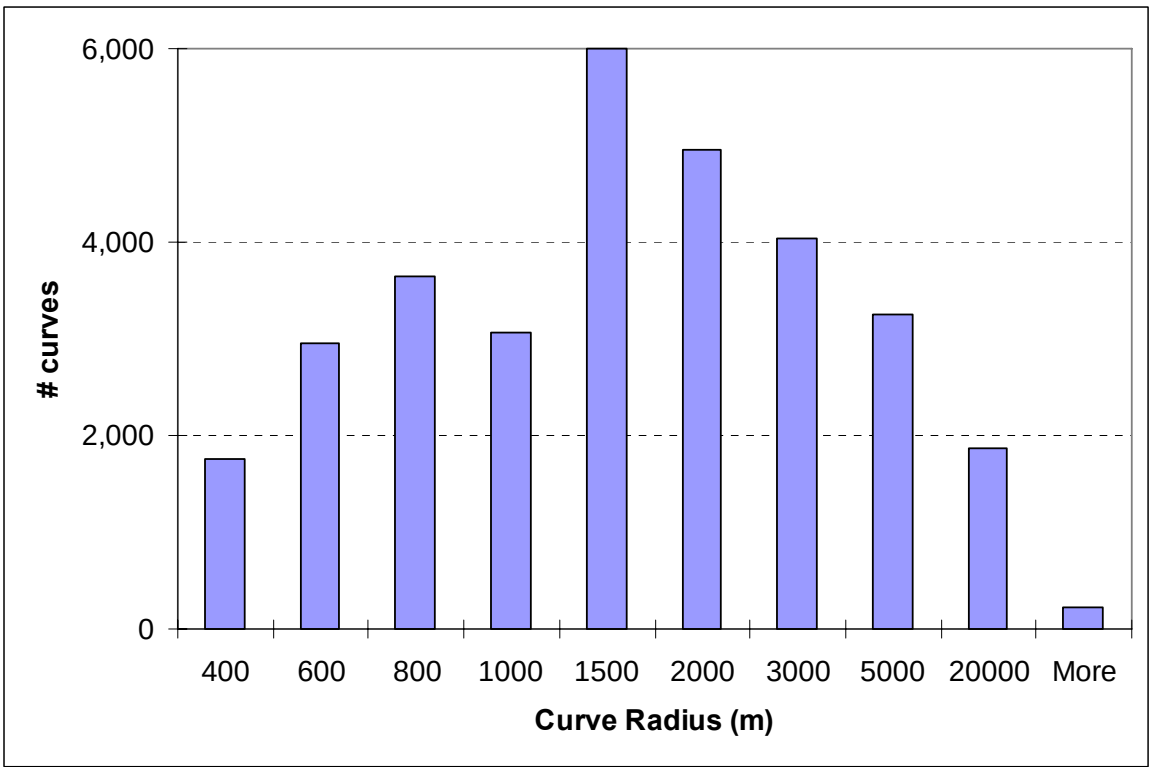

Figure 11. Network Rail Curve Distribution

5.3 Wheel Position

Figure 12 shows the variation of RCF damage with curvature for all four wheels of the lead NACO Swing Motion bogie.

Although it would appear that the wheels on the low rail can cause similar amounts of RCF damage as their counterparts on the high rail, it should be noted that the longitudinal tangential force on the low rail is in the opposite direction to that on the high rail. This means that only the high rail is the driven surface and only this rail is likely to suffer from RCF.

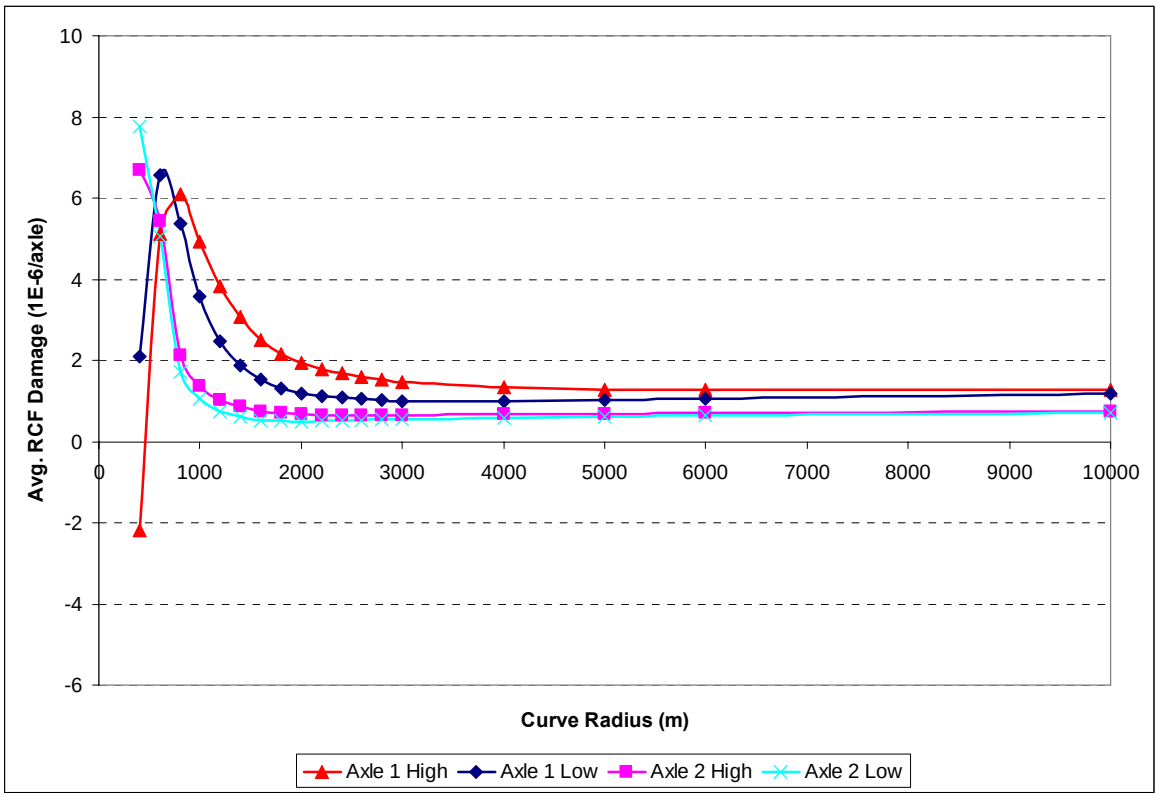

Figure 12. Variation of RCF Damage with Curve Radius – Base Case NACO Swing Motion Bogie, All Wheels, Lead Bogie

For curves with radius greater than 800m, the high rail wheel on the leading axle produces the most RCF damage. For very small radius curves, this wheel can cause wear and it is the high rail wheel on the trailing axle that causes the most RCF damage.

The RCF damage from the high rail wheel on the leading axle has been used in the comparisons that follow.

5.4 Vehicle Type

Figure 13 compares the RCF damage from the high rail wheel on the leading axle of the two locomotives modelled. The Class 60 locomotive has a similar characteristic to the example in Figure 10. The maximum RCF damage from this vehicle arises on curves around 1,400m radius. For smaller radius curves wear becomes more dominant than RCF damage. The steering forces on larger radius curves are insufficient to cause RCF damage.

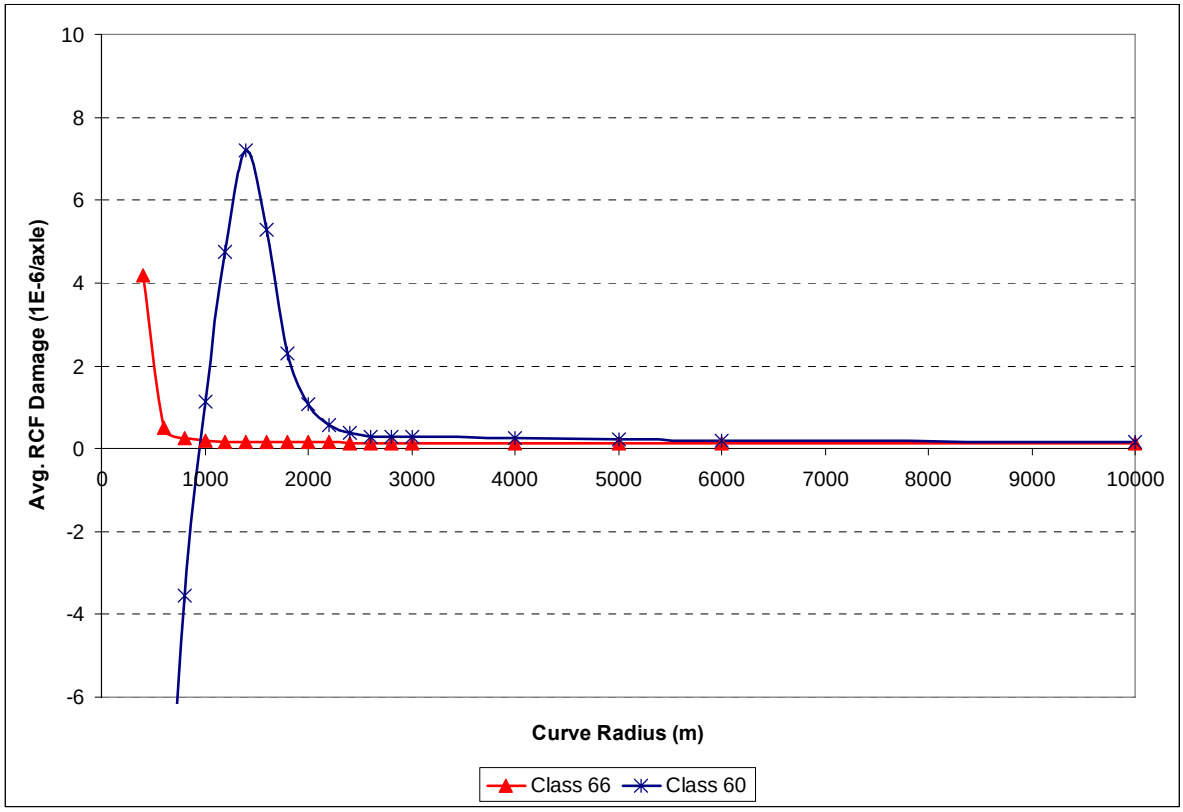

Figure 13. Variation of RCF Damage from Locomotives with Curve Radius – High Rail Wheel, Leading Axle

The Class 66 locomotive has a linkage between the opposite wheels of the leading and trailing axles. This helps to align the axles in a radial position in curves and reduces lateral creep forces. The results in Figure 13 show the Class 66 locomotive is expected to produce very little RCF damage except in small radius curves.

Figure 14 compares the damage from all three freight vehicles modelled. In general, the vehicle with the NACO Swing Motion bogies produces the most RCF damage. This is a three-piece bogie (bolster and two sideframes) with no primary suspension. On large radius curves (and even on straight track) this type of bogie can produce longitudinal and lateral creep forces. This is why, for this bogie, the right end of the RCF damage plot in Figure 14 does not reach zero.

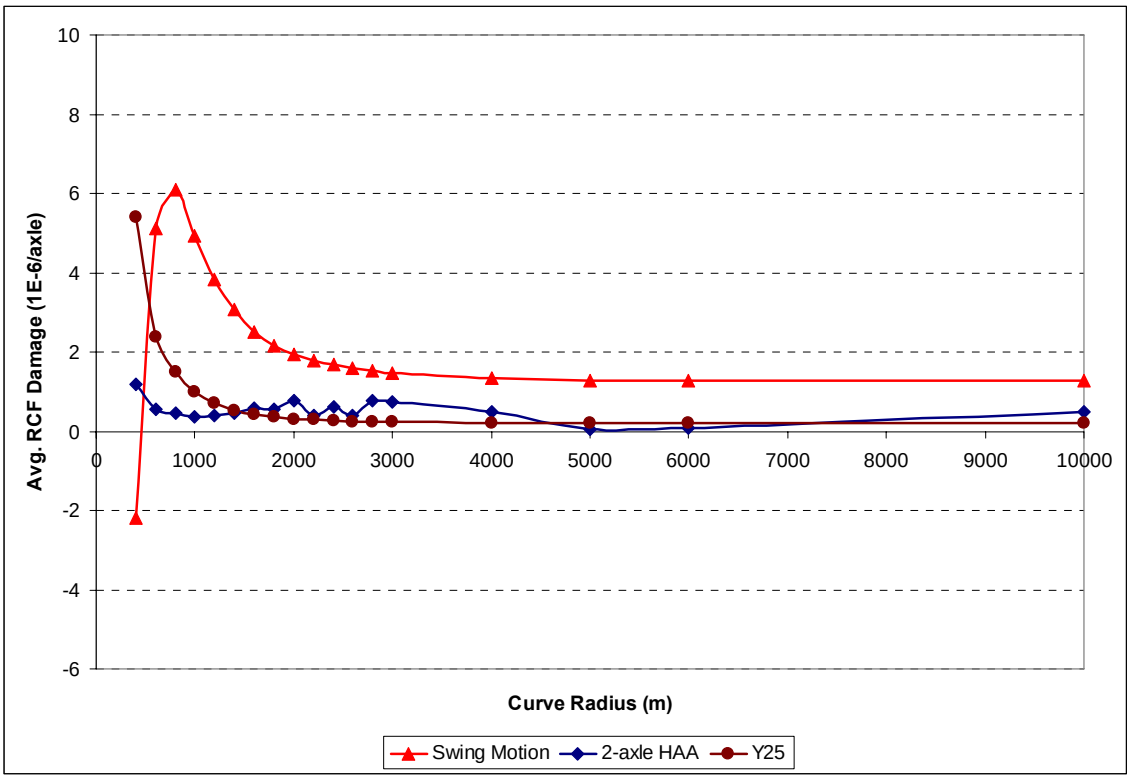

Figure 14. Variation of RCF Damage from Freight Vehicles with Curve Radius – High Rail Wheel, Leading Axle

The Y25 bogie has a solid frame and a primary suspension. The axles are relatively free to move longitudinally until the clearances are taken up in the axle guides. The clearances are ± 2mm in the as-built condition. This means the axles can align themselves radially in curves of radius 360m or more. It explains why the Y25 results in Figure 14 show very little RCF damage except on small radius curves.

The 2-axle vehicle has a relatively long wheelbase, which tends to produces high steering forces. However, its axles have a relatively low yaw stiffness, which counteracts the effect of the long wheelbase. The simulations with the 2-axle vehicle were all performed at its normal operational speed of 45 miles/hour (the other vehicles were modelled at the speeds shown in Table 5).

Figure 15 shows the typical variation of RCF damage with curve radius for a passenger vehicle. The peak in the RCF damage for this particular passenger vehicle occurs at 800m curve radius. On the smaller radius curves the vehicle does not produce enough wear to completely remove RCF damage. The peak value of RCF damage is 8.3×10^{-6}, which is higher than that for the NACO Swing Motion bogie (6.1×10^{-6}) and the Class 60 locomotive (7.2×10^{-6}). One reason for this is that the passenger vehicle is less affected by the track geometry inputs than the other vehicles. Since there is less dynamic variation, the average can be high, and can approach the maximum of 10^{-5}.

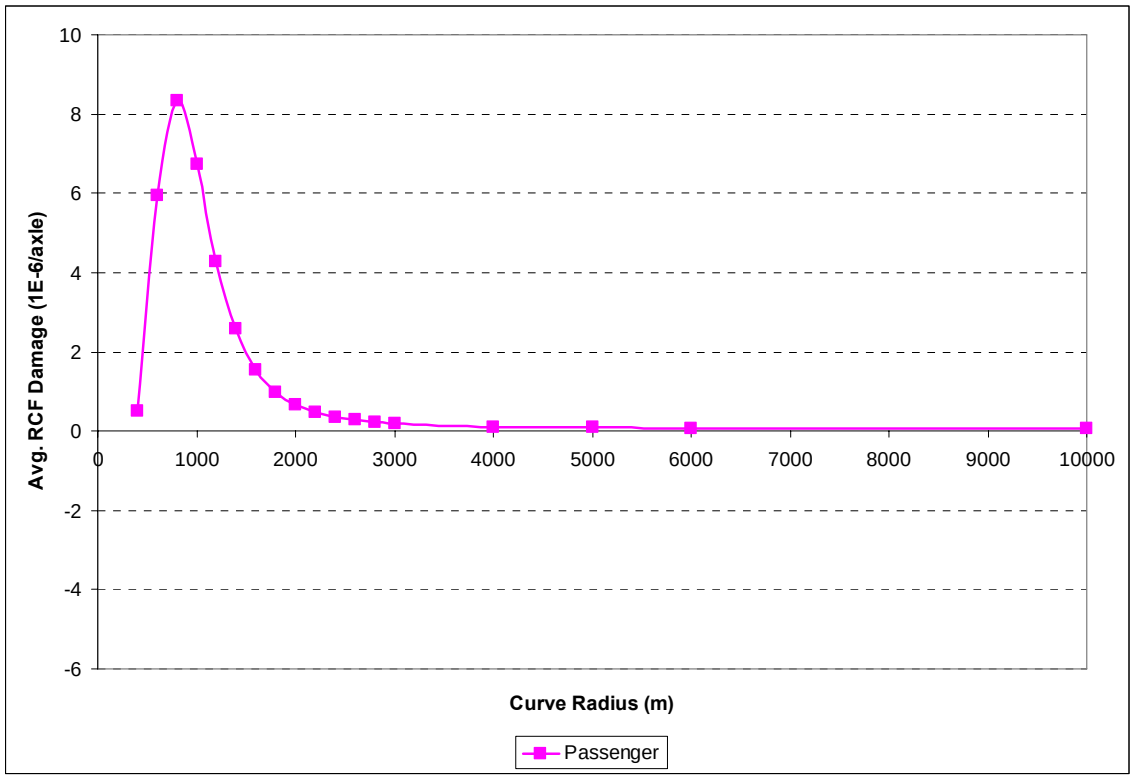

Figure 15. Variation of RCF Damage from a Typical Passenger Vehicle with Curve Radius – High Rail Wheel, Leading Axle

5.5 Track Geometry

Simulations were performed with the Y25 bogie for six different levels of track geometry. Table 8 shows the base-case track input was scaled up and down to give the range of track quality levels.

Table 8. Track Geometry 70m Standard Deviations (mm)

Scale Factor	10%	50%	90%	100%	150%	200%
Vertical	0.4	1.8	3.2	3.6	5.4	7.2
Lateral	0.3	1.6	2.8	3.1	4.7	6.2

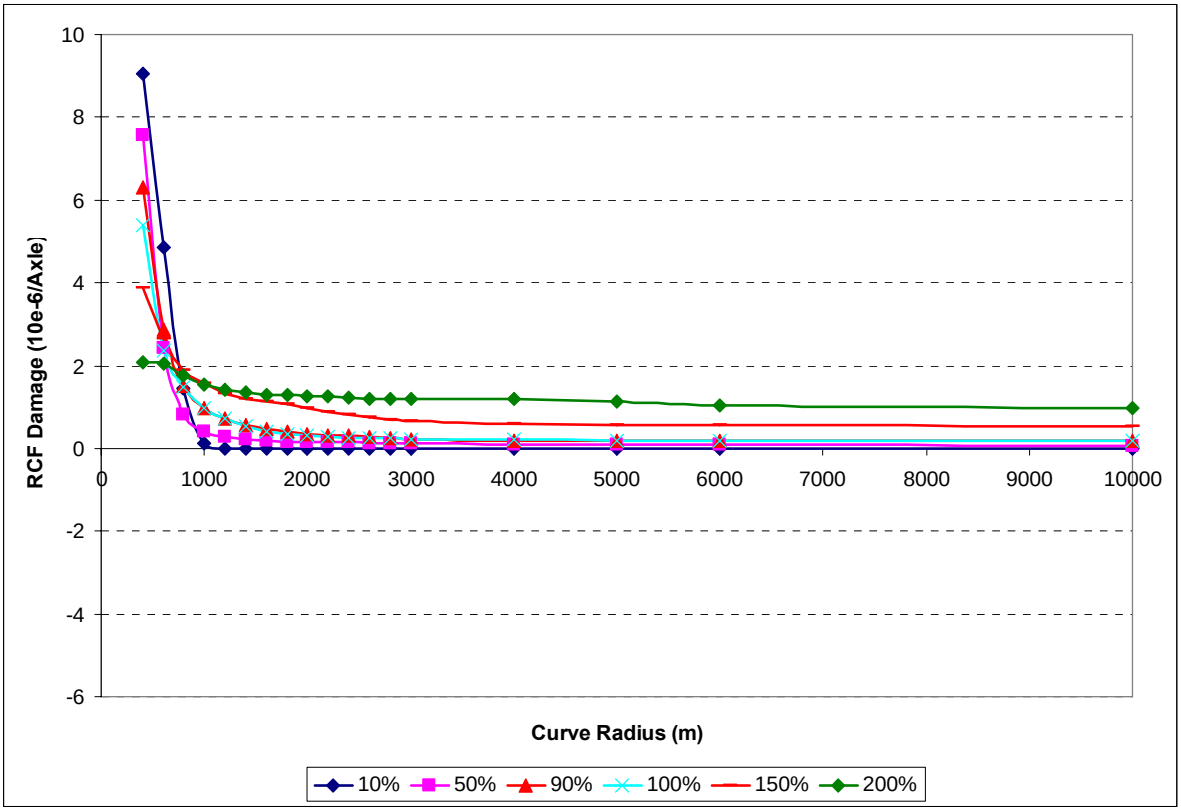

Figure 16. Effect of Track Quality on RCF Damage – FSA with Y25 Bogies

The effect of track quality on the variation of RCF damage with curvature for the Y25 bogie is shown in Figure 16. Increasing track roughness increases tangential wheel/rail forces. For large radius curves this has the effect of increasing the RCF damage. On small radius curves, where some wear is occurring, the effect of increasing track roughness is to increase the wear.

Track quality becomes an important factor to consider when calculating RCF damage if the route in question has a higher than average proportion of small radius curves.

5.6 Conicity

Conicity is a measure of the change in rolling radius difference between two wheels as the axle is displaced laterally. Figure 17 shows the variation in Rolling Radius Difference (RRD) with lateral shift for the worn rails and the worn P8 profiles used in the NACO Swing Motion bogie simulations.

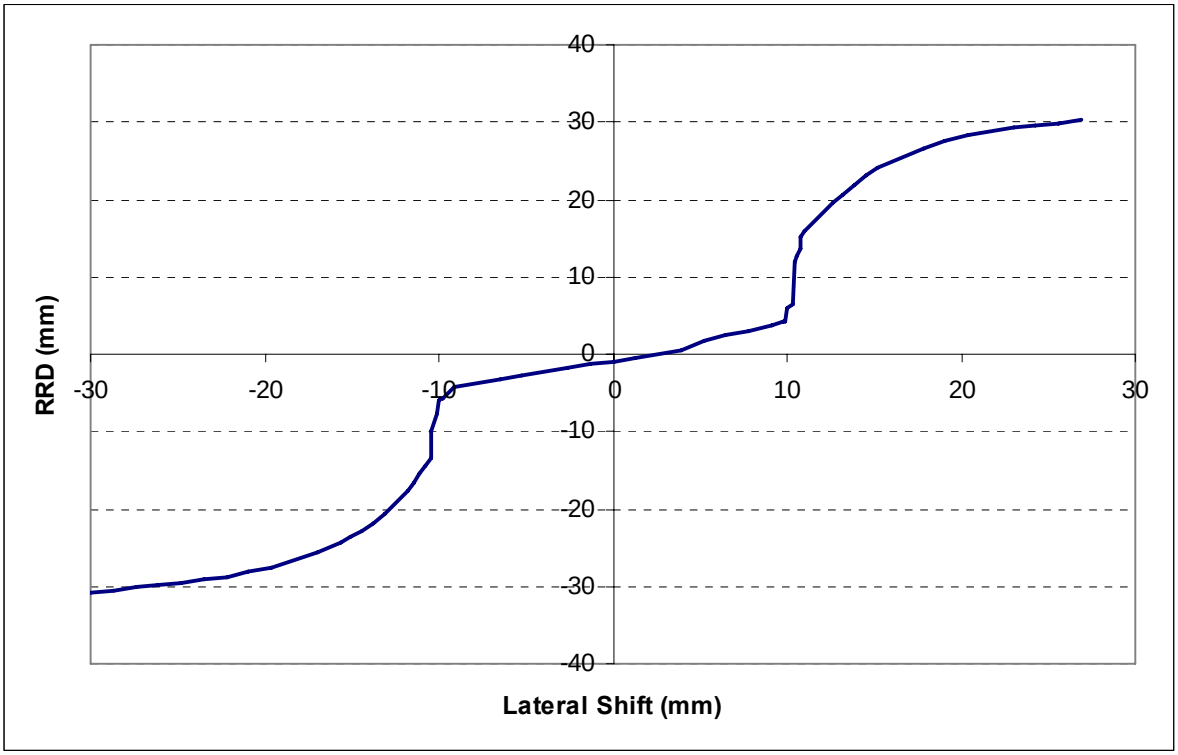

Figure 17. Variation of Rolling Radius Difference with Lateral Shift – Worn P8 Profiles and Worn Rails

Between -10 and +10mm lateral shift, the rolling radius difference varies almost linearly with lateral shift. A straight line fitted to this part of the graph has a slope of 0.46. By definition, the conicity is half this slope, i.e., 0.23 or 23 percent.

The change of characteristic at ±10mm is caused by the contact point on the tread of the wheel moving towards the flange. Flange contact is only expected on curves with small radius.

In general, conicity increases as wheel and rail profiles wear to conformal shapes. Figure 18 compares the RRD plots for three different combinations of wheel and rail profile. Only the part of the plot between flange contacts is shown. The resulting conicities are 12, 23, and 35 percent.

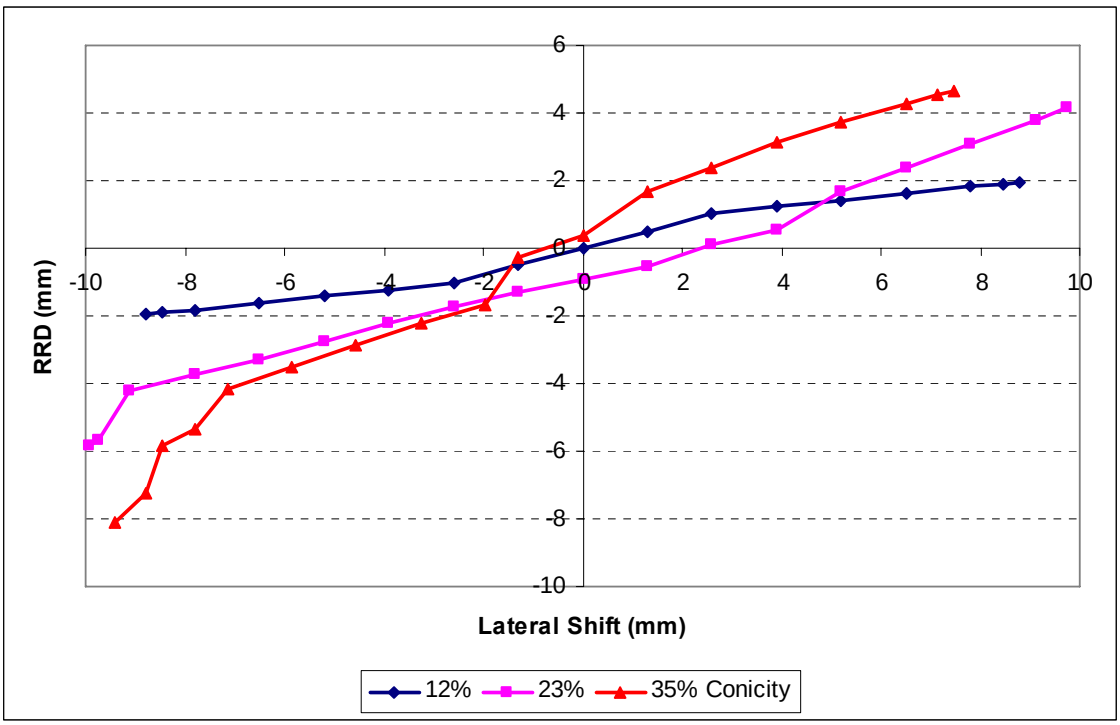

Figure 18. Rolling Radius Difference Plots for Three Wheel/Rail Profile Combinations

Figure 19 shows the effect of conicity on the RCF damage produced by the HTA vehicle with NACO Swing Motion bogies and worn P8 wheel profiles. Reducing conicity results in smaller longitudinal creep forces for the same lateral displacement of the wheelset. On larger radius curves, this has the effect of reducing RCF damage. Low conicity on small radius curves does not allow radial alignment of the axles and results in large lateral creep forces that increase RCF damage.

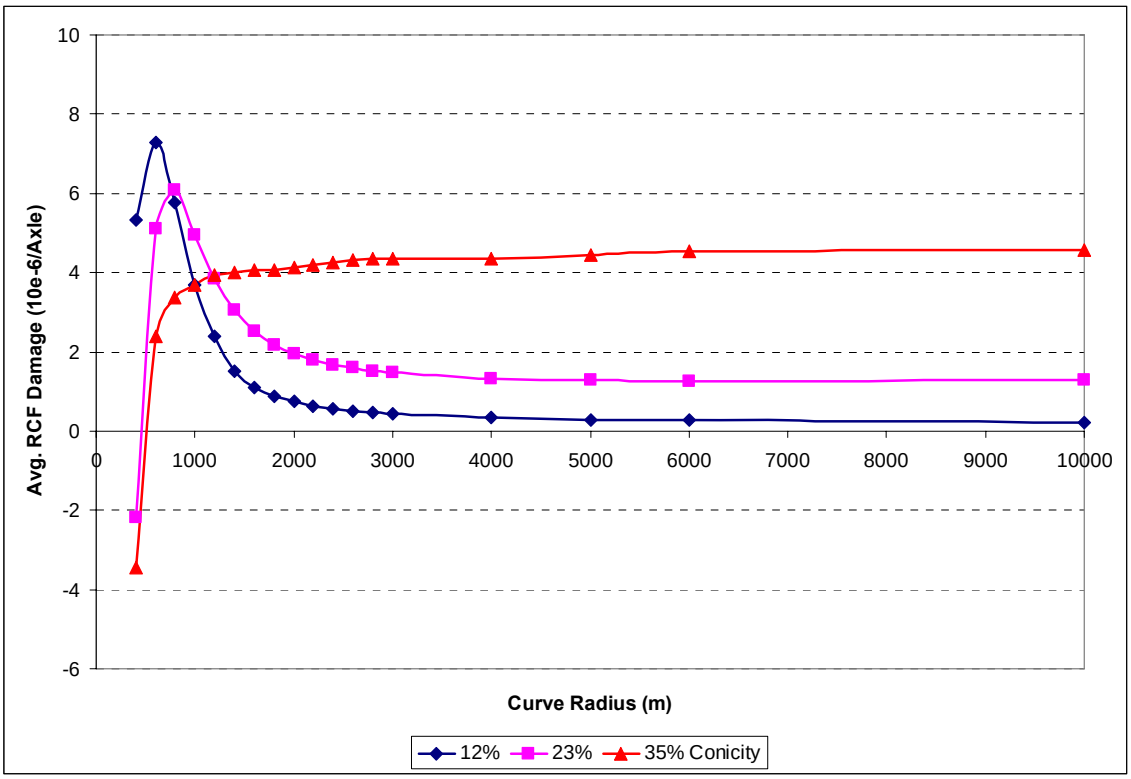

Figure 19. Effect of Conicity on RCF Damage – HTA with NACO Swing Motion Bogies

Increasing conicity improves the ability of wheelsets to steer in all, except the smallest, radius curves. However, for large radius curves, any small offset in wheelset lateral position will result in longitudinal creep forces and RCF damage. Such small offsets could be caused by irregularities in track geometry.

Conicity clearly has a significant effect on RCF damage. Conicity is affected by the profiles of both the wheels and rails. To assess properly the RCF damage for any vehicle would require knowledge of the variation of wheel profile over the vehicle fleet and the distribution of rail profiles on the route over which the vehicle operates.

5.7 Unsprung Mass

Unsprung mass (the mass of the axle wheels and axleboxes) was varied by ±10 percent for the NACO Swing Motion bogies. The effect on the variation of RCF damage with curvature was found to be negligible.

5.8 Bogie Yaw Inertia

Bogie yaw inertia was varied by ±10 percent from the nominal value for both the Y25 and NACO Swing Motion bogies. The effect on the variation of RCF damage with curvature was found to be negligible.

5.9 Primary Longitudinal Clearance

The primary longitudinal clearance is the distance that the axle is free to move in the longitudinal direction on its primary suspension before it makes metal-to-metal contact. For the Y25 bogie, the design value of this clearance is 2mm. The results of varying this value are shown in Figure 20.

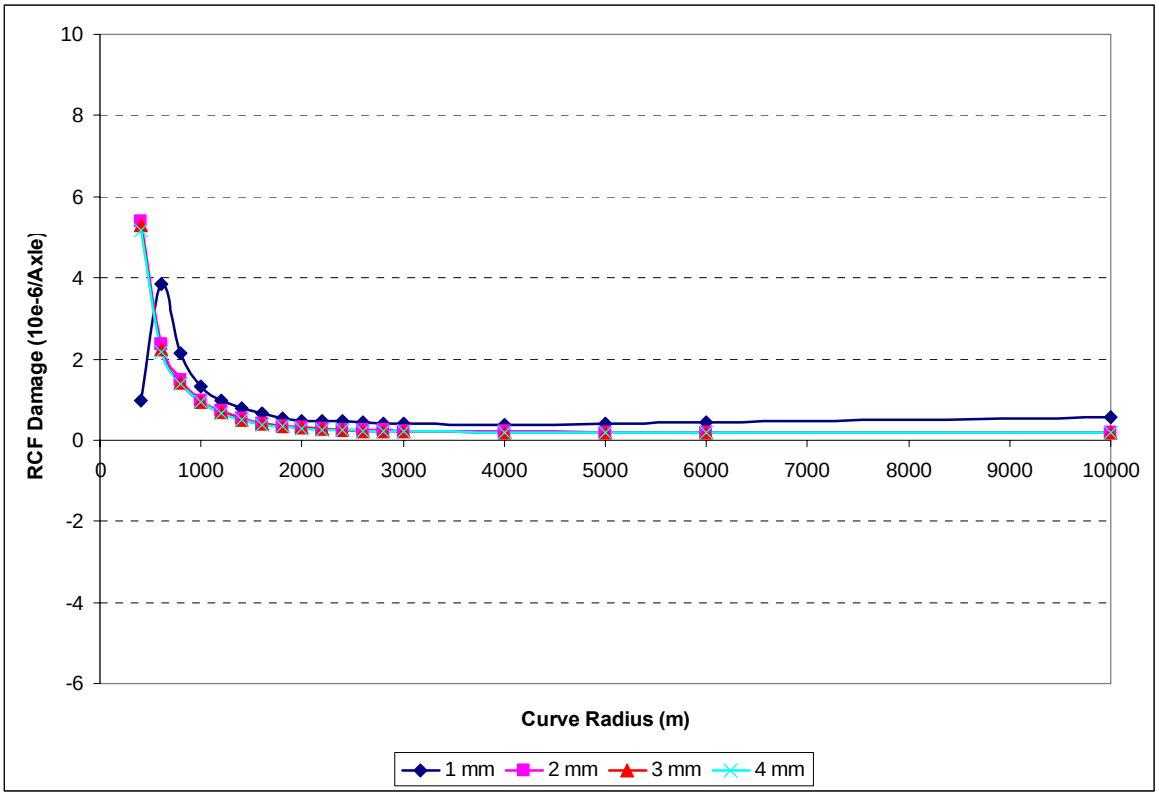

Figure 20. Effect of Primary Longitudinal Clearance on RCF Damage – FSA with Y25 Bogies

Figure 20 shows that increasing the primary longitudinal clearance for the Y25 from its design value has no effect on the variation of RCF damage with curve radius. This indicates that the design clearance is sufficient to allow the axles to steer over the range of curves considered. Increasing the clearance does not improve steering.

When the clearance is reduced to 1mm, variation of RCF damage with curvature changes. RCF damage increases slightly for all curvatures except the one with the smallest radius. For the 400m radius curve, the steering forces increase to a level that causes wear to counteract some of the RCF damage.

Although reducing the clearance increases RCF damage, it is more likely in practice that clearances will increase due to wear. Thus, as a first approximation, it can be assumed that primary longitudinal clearance does not have a significant affect on RCF damage.

5.10 Primary Lateral Clearance

The primary lateral clearance is the distance the axle can move in the lateral direction on its primary suspension before metal-to-metal contact is made. The design value for the Y25 bogie is 10mm. Simulations were performed with this clearance adjusted to 6, 12, and 18mm. No effect was found on the variation of RCF damage with radius of curvature.

The design lateral clearance for the 2-axle HAA wagon is assumed to be 4mm. Figure 21 shows the effect of varying this value on the variation of RCF damage with curve radius.

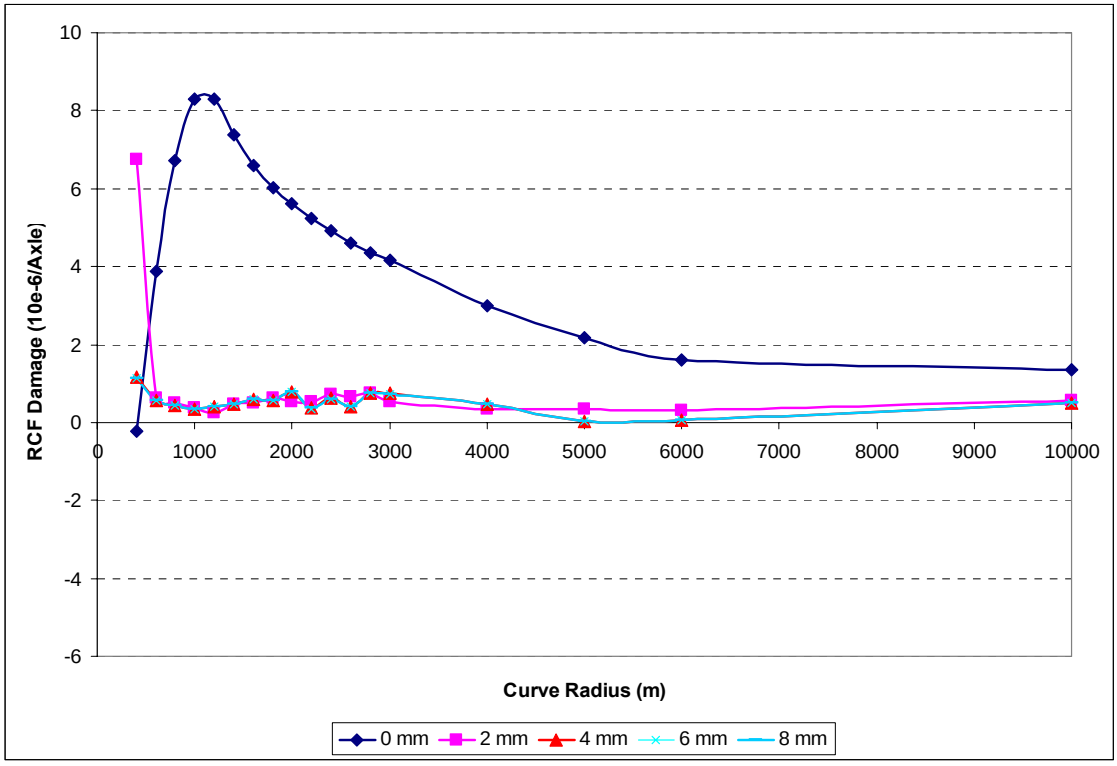

Figure 21. Effect of Primary Lateral Clearance on RCF Damage – 2-axle HAA Wagon

Increasing the primary lateral clearance above the design value for the 2-axle HAA wagon does not affect the RCF damage. When the clearance is reduced to 2mm, RCF damage increases on the smallest radius curve (400m). Closing the clearance completely has the effect of increasing the wheel/rail steering forces for all curvatures. For curves with radius above 1,000m this increases the RCF damage. For curves less than 1,000m the increased steering forces begin to cause wear.

Lateral primary clearance only affects RCF damage if it is reduced to a small value. In practice this clearance is likely to increase from the design value due to wear. Thus, as a first approximation, the effect of primary lateral clearance can be ignored when accessing RCF damage from freight vehicles.

5.11 Primary Yaw Stiffness

Primary yaw stiffness is a constraint between the axles of a bogie or vehicle. It has a significant effect on steering behaviour. The Y25 has a coil spring primary suspension. The springs acting in shear give a longitudinal stiffness between the axles and bogie frame. This longitudinal stiffness applied at the axleboxes produces yaw stiffness between the axle and bogie frame.

In the 2-axle HAA wagon primary yaw stiffness is provided by the longitudinal connection between the axle and body. This connection is made by inclined shackles at the ends of the leaf springs. The nominal value is assumed to be 2MNm/rad. Figure 22 shows the effect of varying this value.

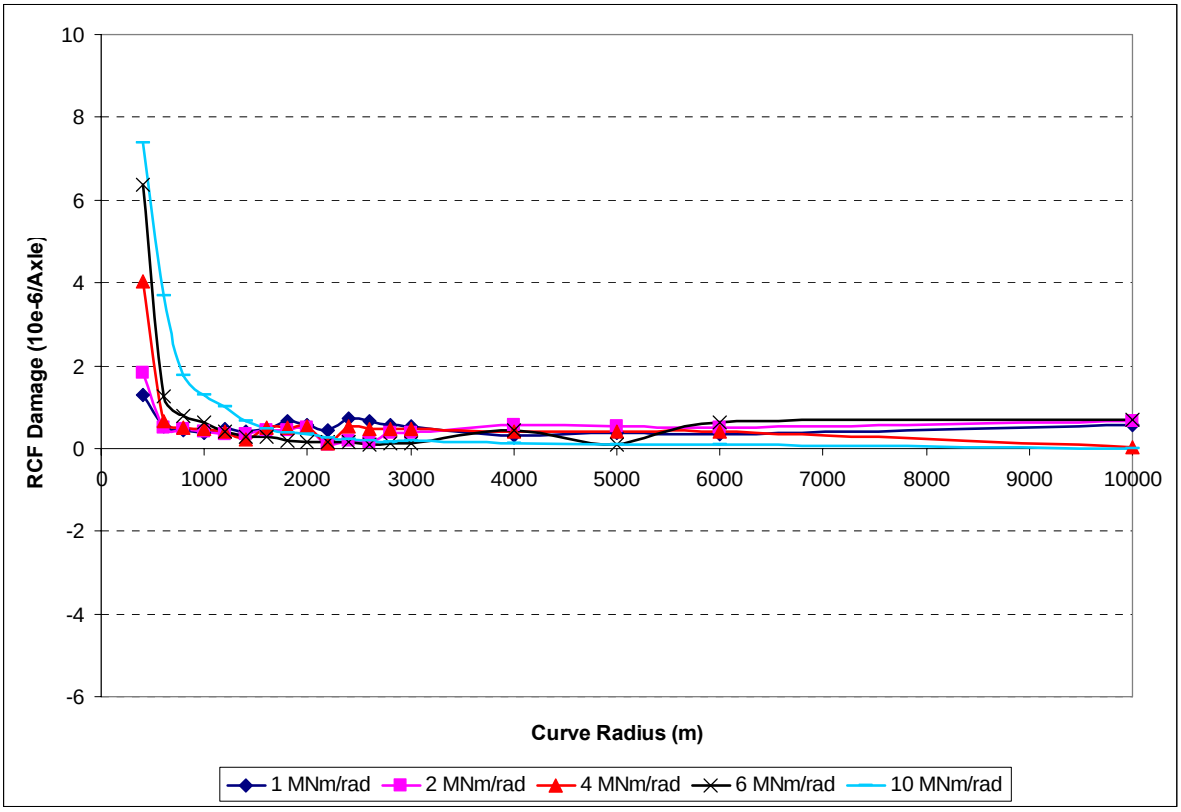

Figure 22. Effect of Primary Yaw Stiffness on RCF Damage – 2-axle HAA Wagon

Primary yaw stiffness can be seen to have an affect on small radius curves. Increasing primary yaw stiffness increases steering forces and increases RCF damage on these curves.

When calculating RCF damage it is important to use an accurate value for primary yaw stiffness if the route under consideration contains a significant proportion of curves with radius less than 1,000m. Primary yaw stiffness can be measured in a simple test in a depot.

Primary yaw stiffness is not a meaningful term for the NACO Swing Motion bogie. This bogie has no longitudinal spring connecting the axle to the bogie frame. Instead it relies on friction between the top of the bearing adapter and the pedestal roof to keep the axle in place. If the friction is overcome, the axle moves a small distance until metal-to-metal contact is made. To model this bogie, it is necessary to know accurately the friction levels and clearances.

5.12 Axleload

Figure 23 shows the effect of axleload on the damage produced by the FSA vehicle with the Y25 bogies. The results are very similar for the fully loaded and 50 percent loaded cases. This is understandable because RCF damage is driven by tangential and not vertical forces. As long as the steering behaviour is not affected by the load then neither should the RCF damage.

When the load is removed (the vehicle is empty), the steering behaviour is affected on large radius curves. The result is higher RCF damage on these curves compared to the loaded cases. The same effect is seen in the simulations with the HTA vehicle fitted with NACO Swing Motion bogies.

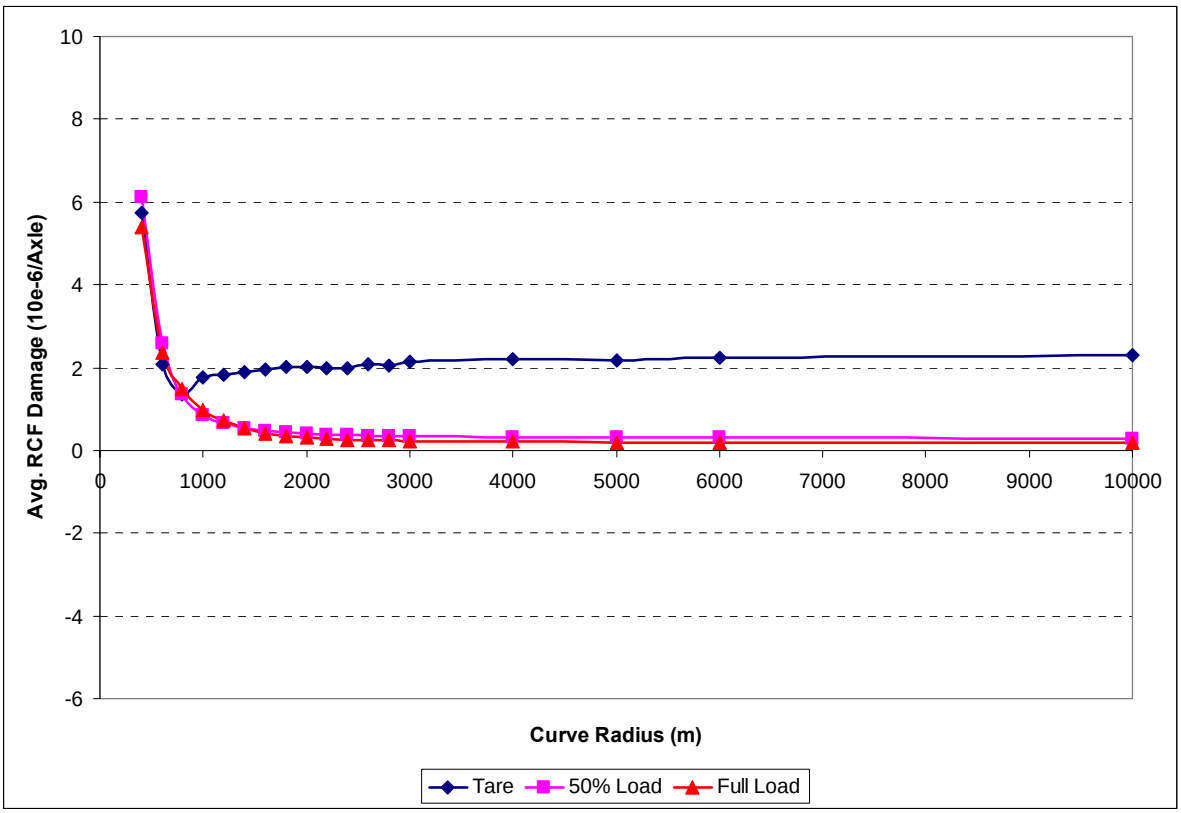

Figure 23. Effect of Axleload on RCF Damage – FSA with Y25 Bogies

In assessing rail surface damage caused by freight vehicles it will be necessary to perform calculations in the tare and laden conditions and combine the results. It would be sufficient to assume only one laden condition.

5.13 Bogie Spacing

The standard bogie spacing of the HTA with NACO Swing Motion bogies (12.72m) was varied by ±10 percent. This was found to have no significant effect on the variation RCF damage with curve radius.

5.14 Axle Spacing

The standard axle spacing of the NACO Swing Motion bogies on the HTA (1.73m) was varied by ±6 percent. As shown in Figure 24, this was found to have a slight effect on the variation of RCF damage with curvature. In comparison with some of the other parameters this effect is not considered significant.

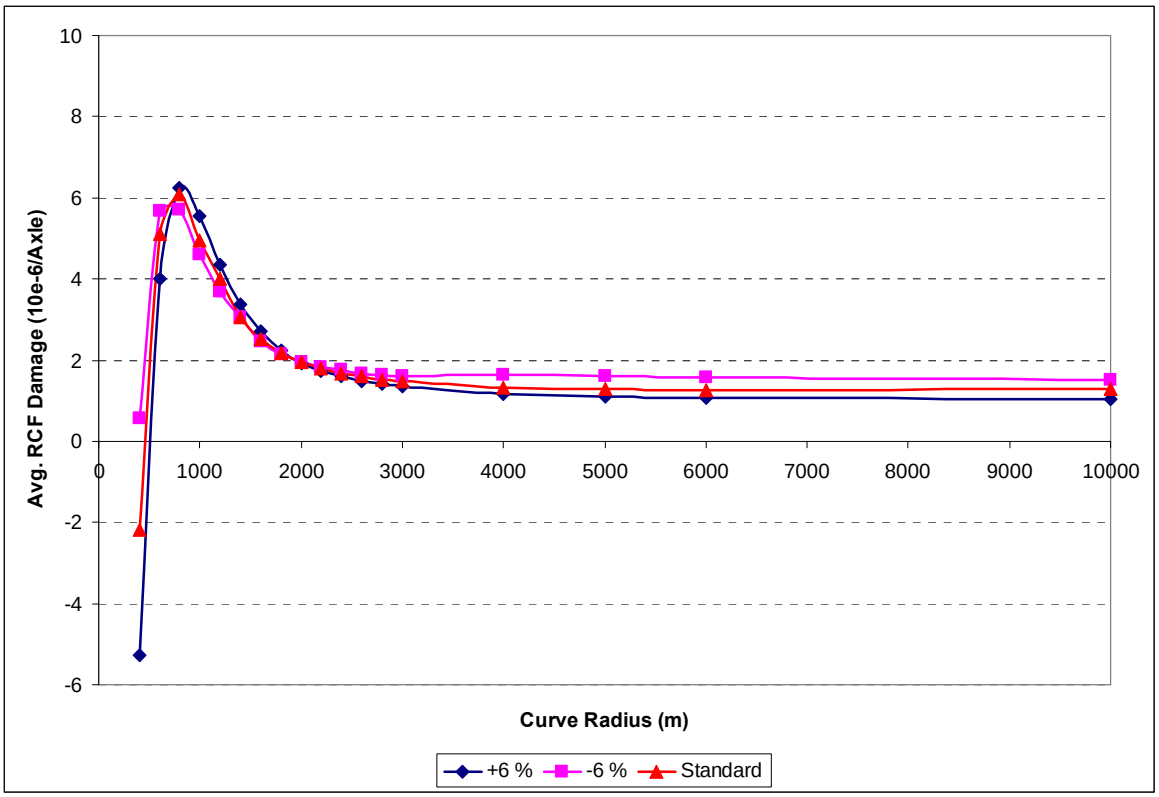

Figure 24. Effect of Axle Spacing on RCF Damage – HTA with NACO Swing Motion Bogies

5.15 Side Bearing Clearance

The NACO Swing Motion bogie has side-bearings between the bolster and wagon body. These carry load when there are net lateral forces producing a roll moment on the wagon body. The side-bearings should be maintained to allow 12mm of vertical movement before metal-to-metal contact in made. Figure 25 shows the effect of changing this tolerance on the variation of RCF damage with curve radius. In these simulations the same variation was applied at each side-bearing.

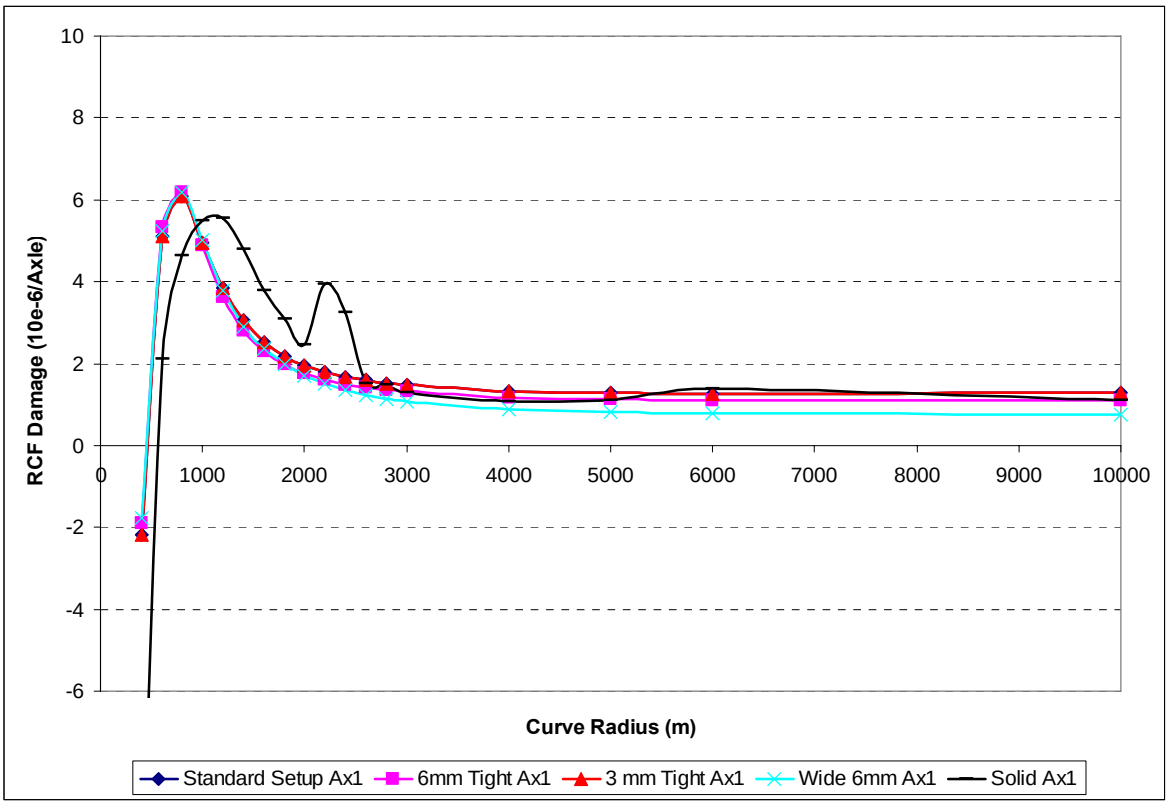

Figure 25. Effect of Side Bearing Clearance on RCF Damage – HTA with NACO Swing Motion Bogies

Altering the side-bearing clearance is seen to have little effect on RCF damage unless the clearance is reduced to zero (solid side-bearings). With zero clearance the steering forces increase on curves less than 2,500m radius. For curves with radius between 1,000m and 2,500m this increases the RCF damage. For curves less than 1,000m radius the increase in steering forces produces wear, which counteracts some of the RCF damage.

Maintaining side-bearing clearances is part of the standard bogie maintenance procedure. If it can be assumed that it is very rare that a bogie is in service with solid side-bearings, then side-bearing clearance need not be considered when evaluating RCF damage from freight vehicles.

5.16 Traction and Braking

The results of the simulations with braking and traction for the Class 60 and Class 66 locomotives are shown in Figures 26 and 27 respectively. Braking was applied to give a deceleration of 10 percent g. Traction was applied to give an acceleration of 10 percent g.

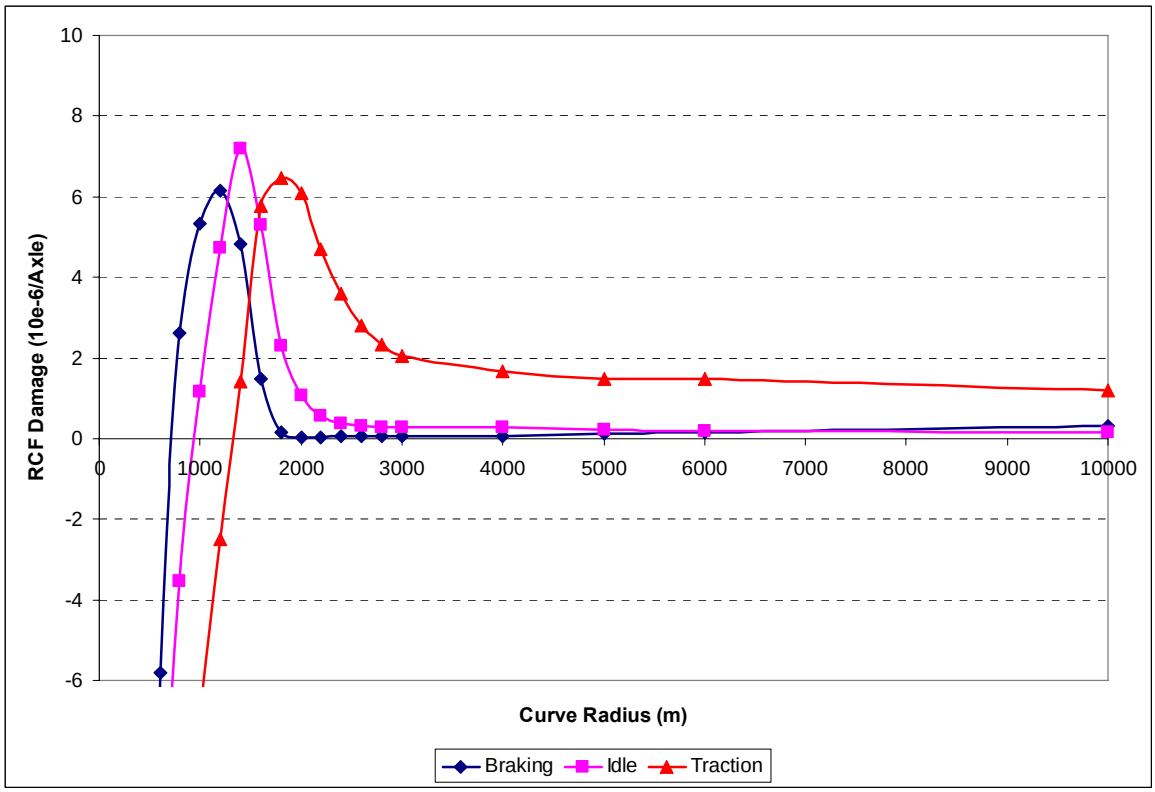

Figure 26. Effect of Braking and Traction on RCF Damage – Class 60 Locomotive

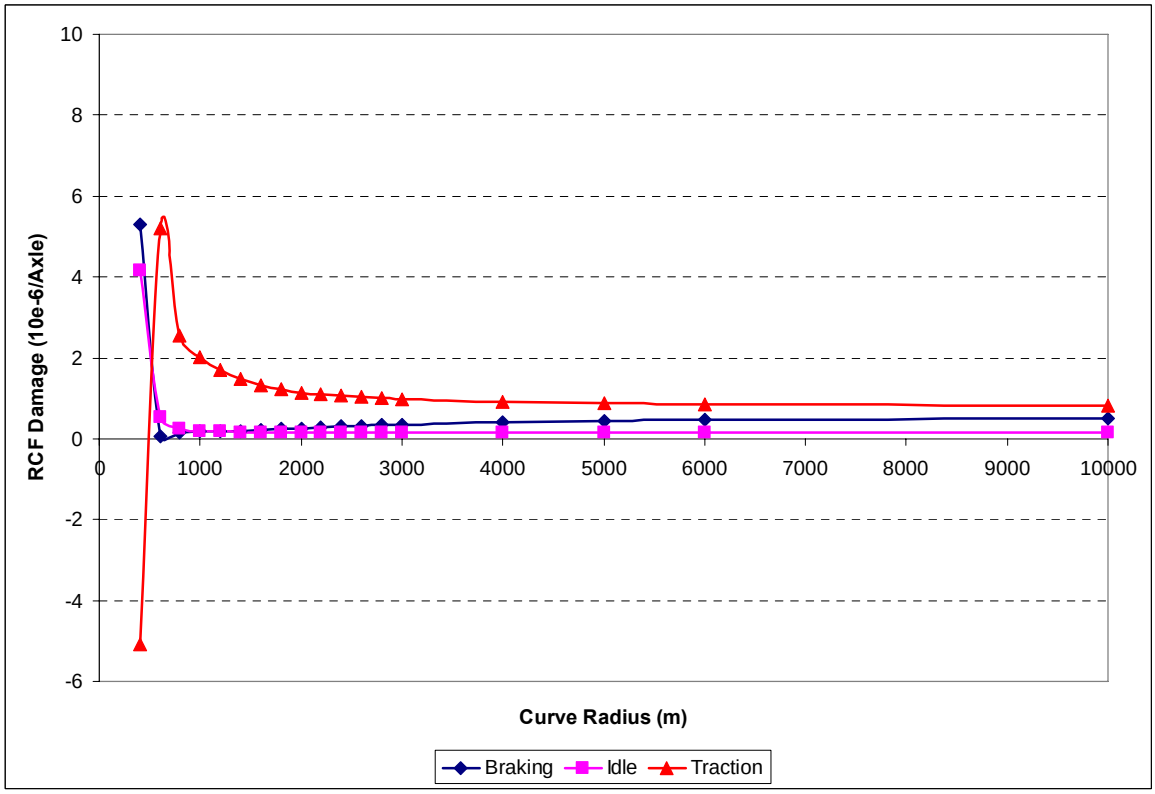

Figure 27. Effect of Braking and Traction on RCF Damage – Class 66 Locomotive

Braking forces act in the opposite direction to the longitudinal steering forces on the high rail in curves. Traction forces add to the longitudinal steering forces on the high rail. Figure 26 shows the two effects. The peak in the variation of damage for the Class 60 locomotive moves to larger curve radii as the sequence of braking to idle to traction is followed.

Braking is seen to have little effect on the RCF damage produced by the Class 66 locomotive. The effect of traction on the Class 66 locomotive is similar to that on the Class 60 locomotive.

The consequences of these results for analysing track access charges depend on the distribution of curves and the gradient profile on the route being considered. For example, if the distribution of curve radius was centred around 2,000m and the Class 60 locomotive was braking or idling when passing through the curves, very little RCF damage would be expected. Alternatively, if the Class 60 locomotive was in traction on those curves, then increased RCF damage would be expected.

6.0 DISCUSSION

6.1 Route-based and Network Charging

In most of the simulations performed in this study the rail surface damage produced by a vehicle was found to vary significantly with curve radius. The distribution of curves varies widely from one route to another. Thus, the same vehicle operating on two different routes can be expected to produce significantly different levels of rail surface damage.

In general, for each type of vehicle there is a particular curve radius that produces the most RCF damage. To base an access charge on this characteristic would be unfair if the vehicle operated on a route that did not contain curves with that particular radius.

Track geometry has been shown to have a significant effect on rail surface damage. Track geometry is maintained to different standards on different routes and is known to vary significantly between freight-only and mixed traffic routes.

Traction and braking have been shown to have a significant effect on the variation of rail surface damage with curvature. Routes with particular combinations of curvature and traction or braking can be expected to incur different levels of rail surface damage than other routes.

The results presented in this report support the argument for route-based evaluation of freight vehicle usage costs. To base a usage charge for freight vehicles on the assumption that they cover the entire network with an average value of traction or braking and average track geometry would be unrepresentative of rail surface damage costs on specific routes.

6.2 Locomotives

An analysis of freight vehicle operational mileages for 2005 has shown that the Class 60 and Class 66 locomotives accounted for 80 percent of all freight locomotive miles travelled. Although these locomotives are similar in appearance they have different steering performance. The Class 66 locomotive has a steering linkage between the leading and trailing axles on each bogie. It produces significantly lower steering forces than the Class 60 locomotive and can be expected to produce significantly less rail surface damage.

On routes with overhead electrification, electric locomotives are likely to cover more mileage than the Class 60 and Class 66 diesel locomotives. It is reasonable to expect there to be significant differences in the steering performance of the different types of electric locomotives.

Thus, if analysing the contribution of freight traffic to track damage at a route level, it is important to consider the actual types of locomotive operating on the route and to accurately model those locomotives.

Traction and braking have been shown to affect the level of rail surface damage produced by locomotives. Thus, it is important to represent traction and braking profiles when modelling these vehicles to calculate rail surface damage.

6.3 Freight Wagons

Analysis of the freight wagon operational data for 2005 shows that there were many different combinations of wagon bodies and bogies in operation. The three most common axle arrangements are the Y25 bogie, single axle leaf spring (2-axle wagon), and NACO Swing Motion bogie. These three account for 58.5 percent of the loaded and 56.1 percent of the empty freight miles.

The Y25 bogie, 2-axle wagon and NACO Swing Motion bogie were modelled in this study. Differences were found in the rail surface damage that each type produced and can be expected in the other types of bogie and axle arrangements that have not been modelled. A full analysis of track damage from freight operations should include other common types of bogie including the Low Track Force bogie and the Gloucester bogie.

A difference was found in the rail surface damage produced by loaded freight wagons when compared to the empty wagons. The variation of rail surface damage under different loads was not found to be significant for the Y25 bogie. Thus, when calculating rail surface damage from freight vehicles, the empty and loaded condition should be considered separately.

Primary yaw stiffness was found to have a significant effect on rail surface damage for curves with radius less than 1,200m. When modelling freight vehicles to calculate rail surface damage it is important to use an accurate value of primary yaw stiffness, preferably one that has been measured.

6.4 Conicity

Wheelset conicity was found to have a significant effect on the rail surface damage produced by freight vehicles. Conicity is affected by the profiles of both the wheel and the rail. A full study of freight vehicle track costs would require information of the variation of wheel profiles over the fleet of vehicles and the variation of rail profiles over the route being considered.

Since the variation of rail surface damage with conicity is significant, it would not be sufficient to assume an average wheel profile and an average rail profile.

6.5 Second Order Effects

The following parameters were studied and found to have an insignificant effect on rail surface damage:

- Unsprung mass (although this is known to be a factor for damage from vertical track forces)
- Bogie yaw inertia
- Longitudinal and lateral primary clearance – assuming it does not become less than the design value. Whilst these clearances do not significantly affect rail surface damage, they may affect high speed stability. The latter has not been evaluated in this study
- Bogie spacing
- Axle spacing
- Side-bearing clearance – assuming it does not become solid

In the simulations performed for this study the vehicles have been assumed to be symmetrical. In practice, vehicles are likely to be constructed with variations in dimensions. For example, tolerances in castings can result in axle misalignment. Further studies could be performed to evaluate the effects of dimensional variations on rail surface damage.

Similarly, when parameters such as side-bearing clearance have been varied in this study, the variations have been applied symmetrically to the vehicle (i.e., all side-bearings were given the same clearance). Further studies could be performed to evaluate the effects of asymmetric parameter variations on rail surface damage.

7.0 CONCLUSIONS

A preliminary study has been made of the effects of several freight vehicle parameters on rail surface damage (wear and rolling contact fatigue). Some parameters were found not to have a significant effect. The parameters that clearly need to be considered when evaluating rail surface damage from freight vehicles are:

- Curve distribution – rail surface damage varies significantly with curvature. The distribution of curve radius on a route will determine the level of rail surface damage it experiences.
- Track quality – rougher track quality generally increases wheel/rail tangential forces and increases either rolling contact fatigue or wear.
- Conicity – variations in wheel and rail profiles can produce significantly different rail surface damage, all other things being equal.
- Vehicle type – there are significant differences in rail surface damage from different types of freight locomotives and wagons. The characteristics of each one needs to be known and modelled. Primary yaw stiffness in particular should be determined accurately.
- Empty or loaded – both of these conditions need to be considered when evaluating rail surface damage from freight vehicles.
- Traction and braking – both can make a significant difference to rail surface damage depending on the distribution of curve radii.

Several of the parameters listed above vary from route to route in the network. This leads to the conclusion that to calculate and allocate the effect of freight traffic on rail surface damage accurately will require a route-based charging regime. Since passenger trains also contribute to the surface damage of rail, the same conclusion applies to passenger rolling stock.

Accurate route-based allocation of rail surface damage on the infrastructure controlled by Network Rail would require development of vehicle and bogie computer models that reflect the characteristics and performance of the many different designs in operation. It would also require development and maintenance of accurate track and vehicle condition databases.

REFERENCES

1) Network Rail, October 2005. “Inspection and Maintenance of Permanent Way,” *Network Rail Standard MR/SP/TRK/001*, Issue 02, London, UK.

2) M. Burstow, October 2003. “Whole Life Rail Model Application and Development for RSSB – Development of an RCF Damage Parameter,” *AEATR-ES-2003-832.* Issue 1, Rail Safety & Standards Board, London, U.K.

APPENDIX A
FREIGHT LOCOMOTIVES, WAGONS, AND BOGIES – 80TH PERCENTILE UTILIZATION

Table A1. Locomotive Utilization by Miles Driven

Rank	Class	Total Miles	Power	% Total Miles	Cumulative %
1	66	21,091,831	Diesel Loco	64.3	64.3
2	60	4,918,012	Diesel Loco	15.0	79.3
3	92	1,581,502	Electric Loco AC	4.8	84.1
4	86	1,319,655	Electric Loco AC	4.0	88.1
5	90	790,212	Electric Loco AC	2.4	90.5
6	59	658,365	Diesel Loco	2.0	92.6
7	67	645,227	Diesel Loco	2.0	94.5
8	57	589,547	Diesel Loco	1.8	96.3
9	37	551,709	Diesel Loco	1.7	98.0
10	20	329,581	Diesel Loco	1.0	99.0
11	47	237,415	Diesel Loco	0.7	99.7
12	33	17,182	Diesel Loco	0.1	99.8
13	98	16,081	Steam Loco	0.0	99.8
14	87	12,142	Electric Loco AC	0.0	99.9
15	9	11,745	Diesel Loco	0.0	99.9
16	8	10,376	Diesel Loco	0.0	99.9
17	50	7,609	Diesel Loco	0.0	100.0
18	73	6,282	Diesel Electric loco	0.0	100.0
19	56	3,426	Diesel Loco	0.0	100.0
20	89	1,944	Electric Loco AC	0.0	100.0
21	43	1,579	Diesel Loco	0.0	100.0
22	58	862	Diesel Loco	0.0	100.0
23	31	151	Diesel Loco	0.0	100.0

Table A2. Wagon Utilization by Loaded Car Miles

Rank	Type	Bogie Type	Total Miles	% Total Miles	Cumulative %
1	FSA	Y25	32,822,322	9.47	9.5
2	HTA	Swing Motion	29,439,339	8.50	18.0
3	HAA	Single Axle Leaf Spring	26,688,719	7.70	25.7
4	FEA	Y25	23,988,189	6.92	32.6
5	HHA	Low Track Force	15,687,188	4.53	37.1
6	TEA	Low Track Force	13,860,798	4.00	41.1
7	HMA	Single Axle Leaf Spring	11,596,780	3.35	44.5
8	KFA	Y25	10,913,948	3.15	47.6
9	FCA	Swing Motion	9,346,071	2.70	50.3
10	FTA	Y25	7,881,696	2.28	52.6
11	TTA	Single Axle Leaf Spring	7,465,733	2.16	54.8
12	IKA	Unknown	7,296,014	2.11	56.9
13	BBA	Y25	6,914,118	2.00	58.9
14	TDA	Y25	5,651,156	1.63	60.5
15	KTA	Y25	5,271,017	1.52	62.0
16	FGA	Unknown	5,079,786	1.47	63.5
17	FIA	Y25	4,675,388	1.35	64.8
18	FKA	Y33	4,461,452	1.29	66.1
19	PGA	Single Axle Coil Spring	4,403,457	1.27	67.4
20	MEA	Single Axle Leaf Spring	4,282,046	1.24	68.6
21	JHA	Gloucester variants	3,965,168	1.14	69.8
22	PCA	Single Axle Coil Spring	3,932,778	1.14	70.9
23	JGA	Various	3,875,422	1.12	72.0
24	IFA	Single Axle Leaf Spring	3,410,455	0.98	73.0
25	JNA	Various	3,375,968	0.97	74.0
26	FFA	Unknown	3,362,606	0.97	74.9
27	BAA	Y25	3,343,068	0.97	75.9
28	FAA	Y31	2,482,106	0.72	76.6
29	HAD	Single Axle Leaf Spring	2,412,239	0.70	77.3
30	BYA	Swing Motion	2,340,212	0.68	78.0
31	PFA	Single Axle Leaf Spring	2,157,634	0.62	78.6
32	JUA	Y25	2,096,054	0.61	79.2
33	HGA	Single Axle Coil Spring	2,022,621	0.58	79.8
34	SSA	Single Axle Coil Spring	1,555,905	0.45	80.3

Table A3. Wagon Utilization by Empty Car Miles

Rank	Type	Bogie Type	Total Miles	% Total Miles	Cumulative %
1	HTA	Swing Motion	30,445,520	14.64	14.6
2	HAA	Single Axle Leaf Spring	27,606,472	13.27	27.9
3	HHA	Low Track Force	15,902,782	7.65	35.6
4	HMA	Single Axle Leaf Spring	12,021,567	5.78	41.3
5	BBA	Y25	6,904,476	3.32	44.7
6	FSA	Y25	6,497,749	3.12	47.8
7	JHA	Gloucester	4,999,256	2.40	50.2
8	JNA	Various	4,896,964	2.35	52.5
9	MEA	Single Axle Leaf Spring	4,865,035	2.34	54.9
10	PGA	Single Axle Coil Spring	4,528,501	2.18	57.1
11	PCA	Single Axle Coil Spring	3,970,868	1.91	59.0
12	JGA	Various	3,856,033	1.85	60.8
13	FEA	Y25	3,404,944	1.64	62.5
14	BAA	Y25	3,330,109	1.60	64.1
15	HAD	Single Axle Leaf Spring	2,520,816	1.21	65.3
16	JUA	Y25	2,138,216	1.03	66.3
17	HGA	Single Axle Coil Spring	2,061,533	0.99	67.3
18	BYA	Swing Motion	2,038,690	0.98	68.3
19	FTA	Y25	1,694,705	0.81	69.1
20	FIA	Y25	1,624,479	0.78	69.9
21	PAA	Single Axle Coil Spring	1,521,378	0.73	70.6
22	BDA	Y25	1,458,663	0.70	71.3
23	HFA	Single Axle Leaf Spring	1,453,527	0.70	72.0
24	MBA	Swing Motion	1,409,511	0.68	72.7
25	PHA	Single Axle Coil Spring	1,406,323	0.68	73.3
26	KFA	Y25	1,365,426	0.66	74.0
27	JYA	Various	1,361,028	0.65	74.7
28	FAA	Y31	1,318,345	0.63	75.3
29	BEA	Y25	1,239,585	0.60	75.9
30	FCA	Swing Motion	1,222,226	0.59	76.5
31	FGA	Unknown	1,220,383	0.59	77.1
32	JMA	Low Track Force	1,215,054	0.58	77.6
33	IZA	Single Axle Leaf Spring	1,208,004	0.58	78.2
34	BZA	Y25	1,179,650	0.57	78.8
35	BLA	Y25	1,089,006	0.52	79.3
36	KVA	Unknown	1,019,353	0.49	79.8
37	TEA	NACO Super C	994,108	0.48	80.3

APPENDIX B

VEHICLE PARAMATERS

Table B1. Passenger Vehicle Parameters

Masses		Units
Body	29,000	kg
Bogie Frame	2,325	kg
Axle	1,200	kg
Dimensions		
Bogie Spacing	14.2	m
Axle Spacing	2.6	m
Centre of Gravity above Rail	1.6	m
Wheel Radius	0.425	m
Suspension Properties		
Primary Yaw Stiffness	20.0	MNm/rad

Table B2. Class 60 Locomotive Vehicle Parameters

Masses		Units
Body	80,400	kg
Bogie Frame	8,550	kg
Axle	2,640	kg
Dimensions		
Bogie Spacing	13.1	m
Axle Spacing	2.1	m
Centre of Gravity above Rail	2.1	m
Wheel Radius	0.56	m

Table B3. Class 66 Locomotive Vehicle Parameters

Masses		Units
Body	80,300	kg
Bogie Frame	9,030	kg
Axle	2,400	kg
Dimensions		
Bogie Spacing	13.3	m
Axle Spacing	2.1	m
Centre of Gravity above Rail	1.9	m
Wheel Radius	0.53	m

Table B4. FSA/Y25 Vehicle Parameters

Masses	Empty	Loaded	Units
Body	11,500	65,900	kg
Bogie Frame		1,610	kg
Axle		1,410	kg
Dimensions			
Bogie Spacing		13.0	m
Axle Spacing		1.8	m
Centre of Gravity above Rail	0.51	2.0	m
Wheel Radius		0.46	m
Suspension Properties			
Primary Longitudinal Clearance		± 2.0	mm

Table B5. HTA/NACO Swing Motion bogie Vehicle Parameters

Masses	Empty	Loaded	Units
Body	17,675	92,675	kg
Bolster & Side Frames		1,648	kg
Axle		1,335	kg
Dimensions			
Bogie Spacing		12.72	m
Axle Spacing		1.73	m
Centre of Gravity above Rail	1.6	2.11	m
Wheel Radius		0.42	m
Suspension Properties			
Primary Longitudinal Clearance		± 6.0	mm

Table B6. HAA Vehicle Parameters

Masses	Loaded	Units
Body	43,600	kg
Axle	1,335	kg
Dimensions		
Axle Spacing	3.05	m
Centre of Gravity above Rail	1.14	m
Wheel Radius	0.42	m
Suspension Properties		
Primary Longitudinal Clearance	± 4.0	mm